

# Fatigue fracture of nylon polymers

## Part 1 *Effect of frequency*

M. G. WYZGOSKI, G. E. NOVAK, D. L. SIMON\*

*Polymers Department, General Motors Research Laboratories, and  
General Motors Advanced Engineering Staff, Warren, Michigan 48090-9055, USA*

The purpose of this study was to determine the effect of frequency on fatigue crack propagation rates in unfilled nylon polymers. Specifically it was of interest to investigate the frequency dependence under conditions where hysteretic heat generation did not occur. For dry injection-moulded nylon the results demonstrate that a strong frequency dependence exists with higher crack propagation rates at lower frequencies. This indicates that the mechanism of fatigue crack growth at room temperature is primarily one of creep crack growth, especially at frequencies below 1.0 Hz. It is also noted that hysteretic heating causes fracture mode transitions to occur during stable fatigue crack propagation in injection-moulded nylons, even at relatively low cyclic frequencies (5.0 Hz).

### 1. Introduction

Numerous reports on the fatigue fracture of nylons have been described in the literature [1-6]. This includes studies of the initiation of fatigue failure as a function of initial stress level [7], as well as measurements of fatigue crack propagation rates following the fracture mechanics approach [8]. Manson, Hertzberg and co-workers, in particular, have investigated the fatigue fracture mechanisms for nylon polymers and have demonstrated the importance of moisture content and viscoelastic properties in controlling crack propagation rates [4]. These variables influence the degree of hysteretic heating at the crack tip along with other parameters such as the stress level and loading frequency. In spite of the abundant literature there are still some unanswered questions regarding the fatigue fracture of nylons. For example, the effect of frequency on fatigue crack propagation rates is not clearly defined under conditions where hysteretic heating is not significant. Also the influence of glass fibre orientation on fatigue fracture kinetics of injection-moulded nylon parts has not been demonstrated. The present study was therefore undertaken in order to address these issues as well as to compare the fatigue fracture mechanisms for injection-moulded nylons with previous results for reaction-moulded nylon 6 composites [9]. For the latter, crack propagation measurements were conducted at a fixed frequency of 5 Hz. As part of a more detailed investigation of injection-moulded nylons, the loading frequency was varied from 0.1 to 5.0 Hz and a thermography camera was employed to follow temperature changes in the vicinity of the fatigue crack tip. Results for unfilled nylons are presented in this paper whereas the glass reinforced materials will be described in a second report.

### 2. Experimental procedure

#### 2.1. Sample preparation

Injection-moulding grade nylon 6 (Allied Corporation, Morristown, New Jersey), was identified as

XPN 1033. The unfilled nylon 66 resin employed was Zytel 122L from the E. I. duPont Company, Wilmington, Delaware. Both materials were injection moulded into 50.8 mm by 203.2 mm by 3.2 mm end-gated plaques using standard processing conditions. Prior to moulding, all materials were dried under vacuum at 90°C overnight to remove moisture. Following moulding, the plaques were stored in desiccators to maintain their dry-as-moulded condition. Compact tension specimens were cut from the plaques according to ASTM E-647 with dimensions as shown in Fig. 1. Unless otherwise specified the precrack was oriented parallel to the melt flow direction. Precracks were prepared by using a band saw for the initial notch and extending the notch tip with a jewellers saw and a razor cut.

#### 2.2. Fatigue testing

Fatigue crack propagation measurements were carried out under load control using a closed-loop servo-hydraulic testing machine with a minimum to maximum load ratio of 0.1. Frequency was varied from 0.1 to 5.0 Hz. The fatigue crack advance was monitored using an MTI-65 video camera and cassette recorder which also incorporated a time-date generator. The crack area was illuminated with a fibre optics light source and the precise position of the crack tip was located by means of a densitometer accessory in the video analyser system. In addition to the video camera, an infrared imaging radiometer was employed to monitor any thermal changes during the crack propagation experiment. Both an Inframetrics Model 525 and a Model 600 were used in this study. In a number of cases concurrent measurements were taken of the position and temperature of the crack tip for an individual sample. In other cases the fatigue data which were previously obtained were compared with the temperature data from a separate crack propagation experiment.

Crack propagation data were analysed using an

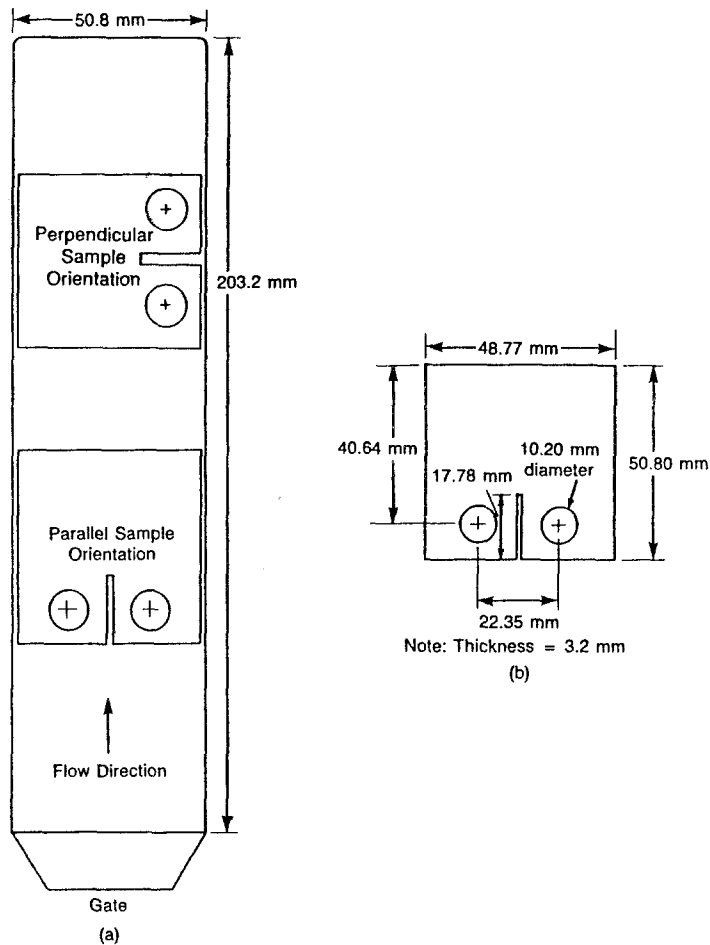


Figure 1 Diagram of injection-moulded plaque showing compact tension sample. (a) Location and orientation, and (b) dimensions.

obtain  $da/dN$  values as a function of crack length, where  $a$  is the crack length and  $N$  the number of fatigue cycles. The crack growth rate data were subsequently plotted as a function of the oscillating stress intensity factor in the usual Paris equation representation of fatigue results.

### 2.3. Fractography

Scanning electron micrographs were obtained of the fatigue fractured surfaces using an ISI Model DS-130 microscope. Comparisons were made of the initiation, propagation, and termination regions of stable fatigue crack growth and the unstable fast fracture at the end of the test.

## 3. Results

### 3.1. Fatigue crack propagation

The fatigue crack growth rates for unfilled injection-moulded nylon 66 as a function of the oscillating stress intensity factor are shown in Fig. 2. Results are given for both orientations of the fatigue crack in relation to the melt flow direction in the plaque. No significant effect of orientation is indicated and both data sets are well fit with a straight line following the usual log-log plot in accordance with the Paris equation

$$\frac{da}{dN} = A(\Delta K)^m \quad (1)$$

where  $\Delta K$  is the oscillating stress intensity factor and the constants  $A$  and  $m$  are evaluated as the intercept and slope of the log-log plot of the Paris equation. Average values from three separate crack propagation

experiments for the nylon 66 were  $A = -6.1$  and  $m = 4.7$  for the parallel orientation.

The fatigue crack growth rate data for injection-moulded nylon 6 were less well behaved as shown in Fig. 3. It is apparent that a systematic variation from the linear regression line occurs with this material. Replicate experiments have demonstrated the reproducibility of this unusual behaviour although the magnitude of the oscillations did vary. It was also noted that the nylon 6 sample exhibited noticeable thinning towards the end of the stable crack propagation region.

Scanning electron microscopy was performed for both types of nylon and results are shown in Figs 4 and 5. The surface features are generally similar to the morphology previously reported for nylons by Bretz *et al.* [1]. However, significant changes were noted here from the initiation of fatigue cracking to the onset of fast fracture. The nylon 66 initially showed a patchy type structure during stable fatigue crack growth; however, this structure underwent a transition to a striated surface more typical of moisturized nylons [2]. The surface striations, equal in spacing to the measured growth rate per cycle, in turn gave way to a more viscous flow toward the termination of the stable crack growth region of the fracture surface. A similar sequence was observed for the nylon 6 except that the initial fatigue crack growth involved a combination of both the patchy and striated surfaces. These results for both nylons, along with the unusual  $da/dN$  data for the nylon 6, suggested that significant crack-tip heating might have occurred during the test. It should be

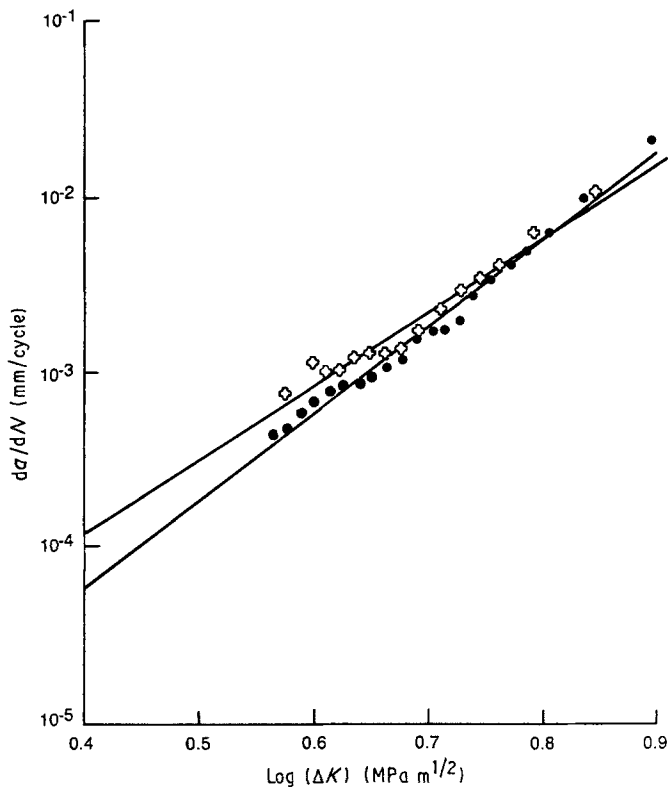


Figure 2 Fatigue crack propagation rates ( $da/dN$ ) for unfilled injection-moulded nylon 66 plotted against stress intensity factor ( $\Delta K$ ) for crack growth (●) parallel or (◻) perpendicular to the melt flow direction.

noted that similarly run fatigue crack propagation experiments at 5 Hz using reaction moulded nylon 6 had shown a constant fracture surface morphology from initiation to termination with no evidence of hysteretic heating at the crack tip [9].

### 3.2. Thermography

To examine the possibility of localized heating in the injection-moulded nylons a thermography camera was employed as previously mentioned. Fig. 6 shows several views of a growing fatigue crack in nylon 66 using a normal video and a thermal imaging camera.

Fig. 6a is a visual shot of the nylon plaque while under test. Fig. 6b shows a thermogram of the sample plaque seen in the far infrared (8 to 14  $\mu\text{m}$ ) region of the electromagnetic spectrum. Fig. 6c shows a black and white photo of what was originally a colour enhanced thermogram under conditions where significant crack-tip heating is occurring. The enhancement of the varying grey scales clearly reveals the increasing temperatures in the vicinity of the fatigue crack tip. Isothermal contours, which are normally colour enhanced, could also be provided as shown in Fig. 6d. Using this feature and by precisely varying the thermal level

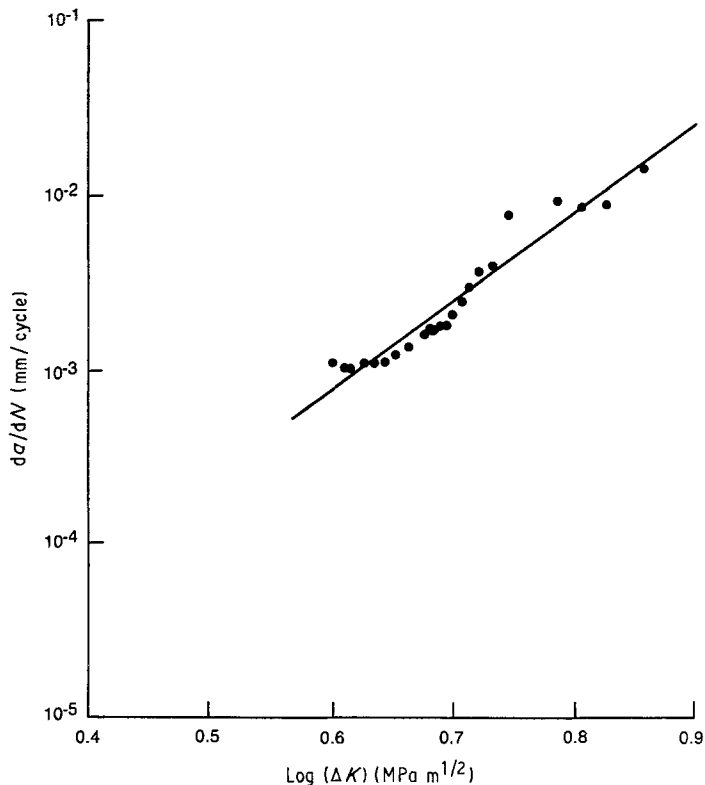


Figure 3 Fatigue crack propagation rates ( $da/dN$ ) for unfilled injection-moulded nylon 6 plotted against stress intensity factor ( $\Delta K$ ).

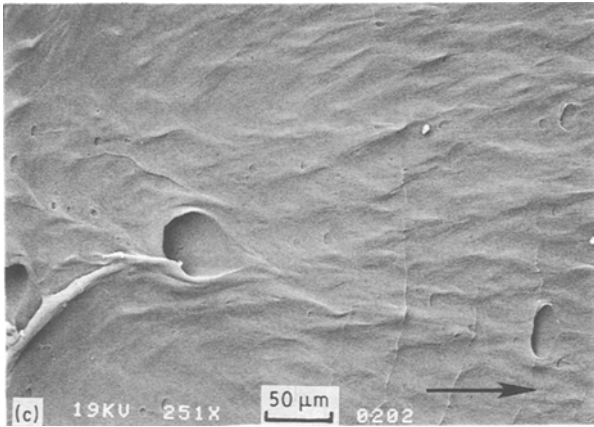
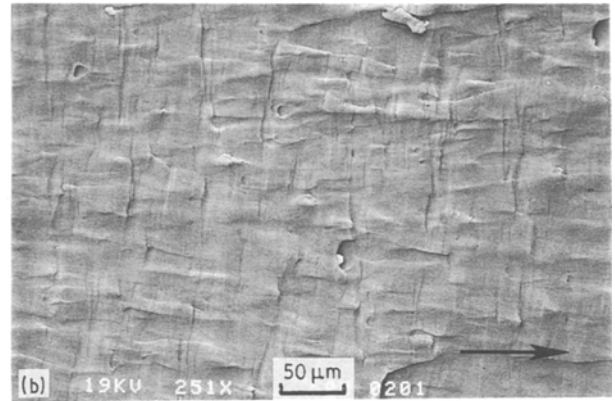
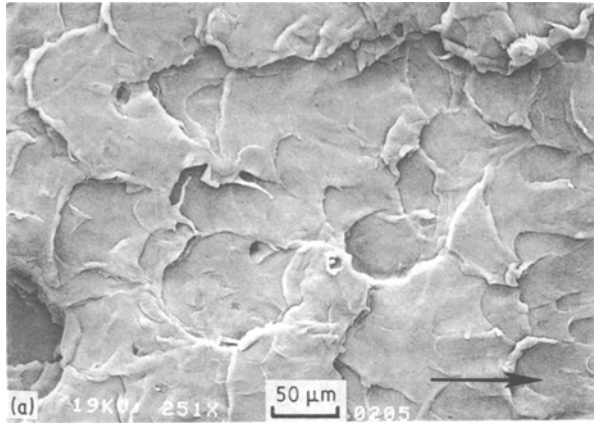


Figure 4 Fatigue fracture surface of nylon 66 tested at 5 Hz showing (a) patchy structure at the start, (b) striations at the midpoint, and (c) viscous flow near the termination of the stable crack growth region.

settings it was determined that the maximum temperature on the specimen occurred at the visually observed crack tip.

The temperature analysis was performed on the video-recorded infrared image. This involved the selection of a horizontal position on the test sample to obtain a thermal cross-section along the growing

fatigue crack. Fig. 7a illustrates the location of the line scan and Fig. 7b shows the full screen display of the actual temperature readings along the line selected. From this figure one can assess the size of the heated zone during the fatigue crack propagation measurement. The highly localized nature of the hysteretic heating phenomenon presumably corresponds to the stress distribution at the crack tip coupled with the heat dissipation away from this region. For the present study the peak temperatures (at the crack tip) were determined and compared with the crack growth rate data which in turn are expressed in terms of the maximum stress intensity factor.

Before introducing this comparison, it is worth pointing out some other observations concerning the crack-tip temperature during the fatigue experiment. For example, during the slow playback mode of the recorded infrared image, heat pulsations of the order of a few degrees were observed at the same frequency as the oscillating tensile load on the sample. Thus it was possible to measure a crack tip temperature for both the crack open as well as the crack closed positions during the test. Fig. 8 shows the temperature at the crack tip for a nylon 66 sample cycled at 5 Hz.

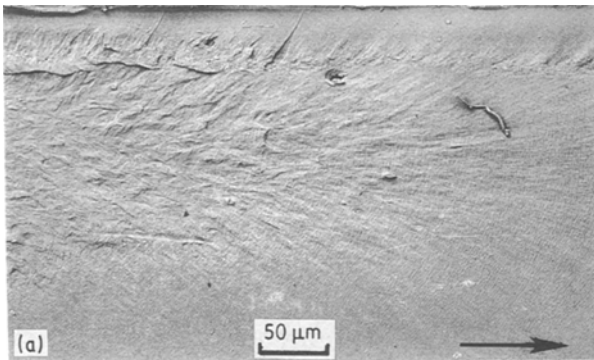
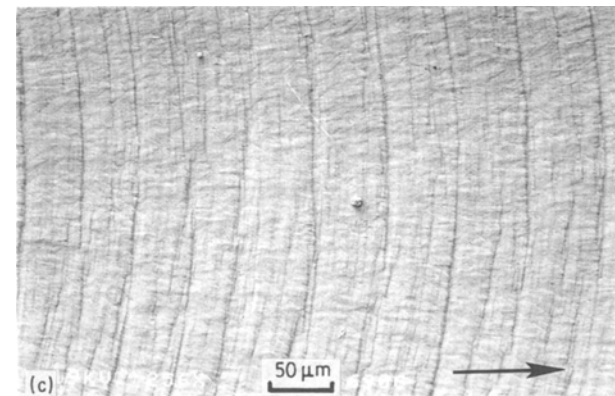
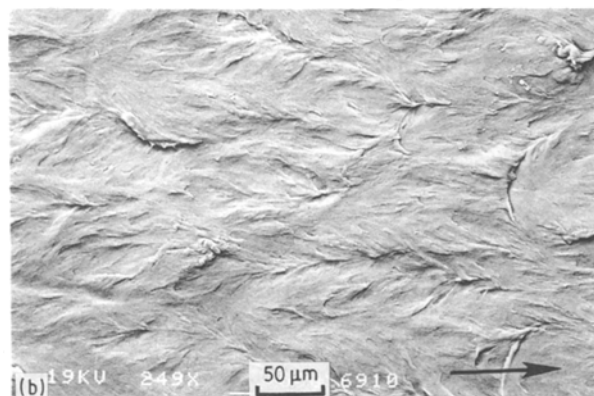


Figure 5 Fracture surface of injection-moulded nylon 6 showing (a) combination of patchy type structure and fatigue striations ( $\times 17.5$ ), (b) higher magnification views of patchy structure and (c) fatigue striations. Crack growth direction is shown by arrows in this and all subsequent figures.



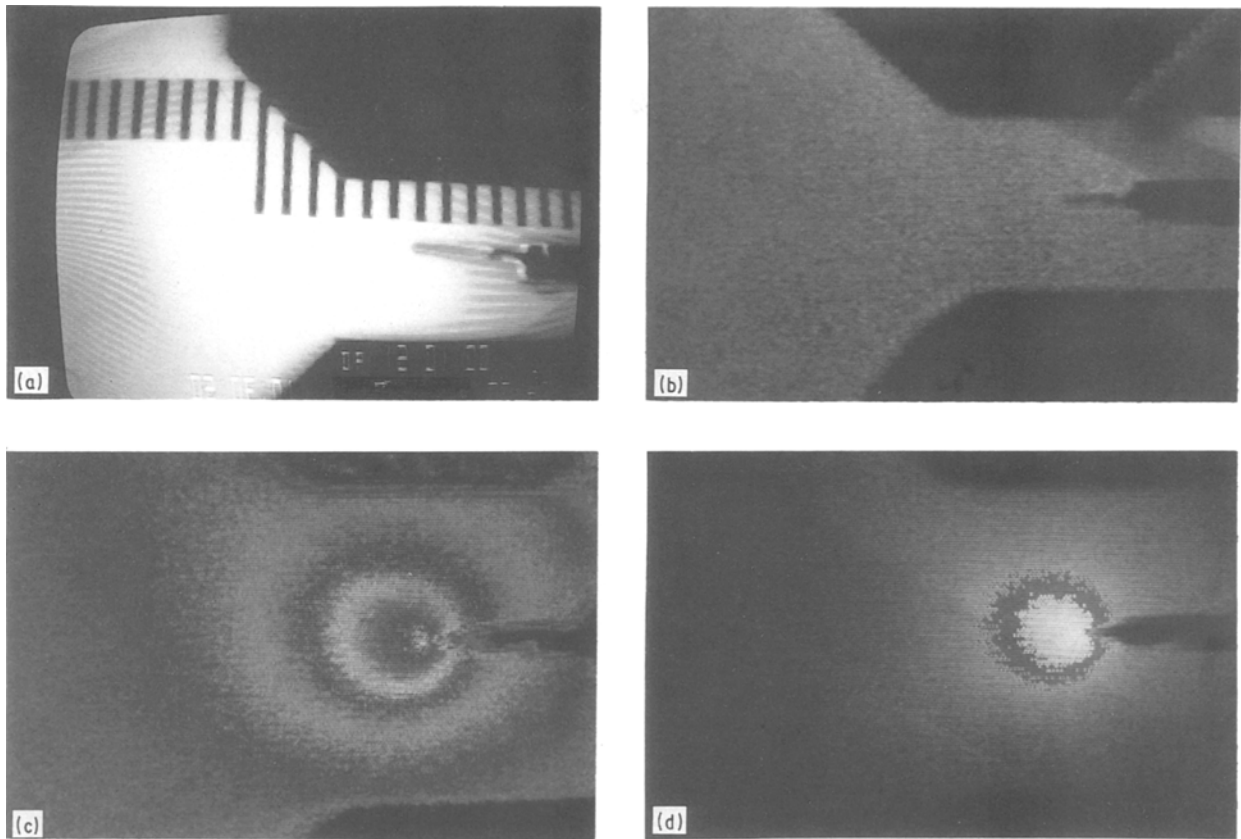


Figure 6 Images of a growing fatigue crack in a nylon sample ( $\times 2.4$ ): (a) normal video image, (b) thermogram seen in the far infrared region, 8 to 14  $\mu\text{m}$ , (c) colour-enhanced thermogram, (d) colour-enhanced isothermal contours of the same sample.

Note that the higher temperature occurred for the crack closed position (minimum stress) rather than the crack open position (maximum stress). This is not the anticipated trend if all of the temperature change were attributed to hysteretic heating. The unexpected inversion in temperature with loading is believed to be a manifestation of the thermoelastic effect which has been reported by others to occur in polymers [10]. Simply stated the thermoelastic effect requires that solid materials will cool when put under a tensile stress and will experience a corresponding heating under a compressive stress. This is, of course, the opposite of what is expected from hysteretic heating alone. The fact that the thermoelastic cooling can be measured while superposed upon the hysteretic heating provides evidence of the accuracy of the thermography technique.

Although not clearly shown in Fig. 8, it was also

noted that near the very end of the fatigue test a reversal in temperature for the open and closed positions occurred. Thus at the highest stress intensity levels the higher temperatures were measured for the crack open position. This could be due to the increased magnitude of the hysteretic effect, but also may suggest that the region in the vicinity of the crack tip is experiencing a compressive loading owing to the high degree of bending at the termination of the fracture of the compact tension sample [11]. These observations demonstrate that both an elastic and a viscoelastic temperature change occur at the fatigue crack tip; however, it is the latter effect which predominates as the crack propagates at accelerated rates toward the end of the test. In the following discussion all reported temperatures, as well as all crack growth rate data, represent measurements taken from the video recordings with the crack tip in the fully open position.

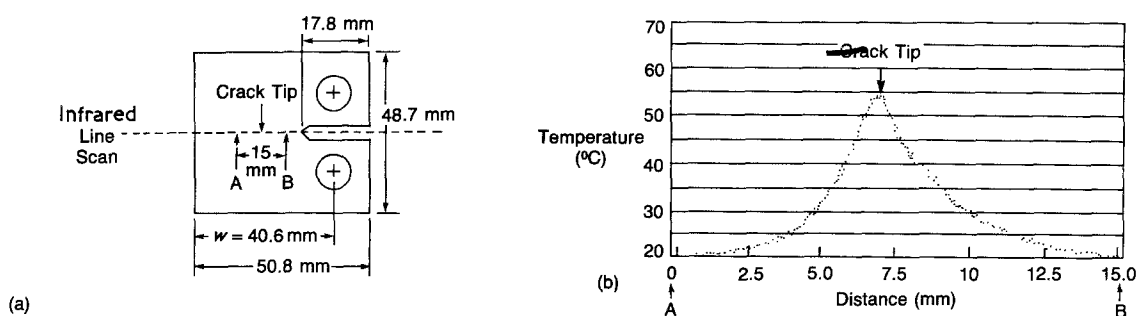


Figure 7 Dimensional layout of compact tension sample showing (a) crack tip position and infrared line scan, and (b) temperature distribution along the infrared line scan.

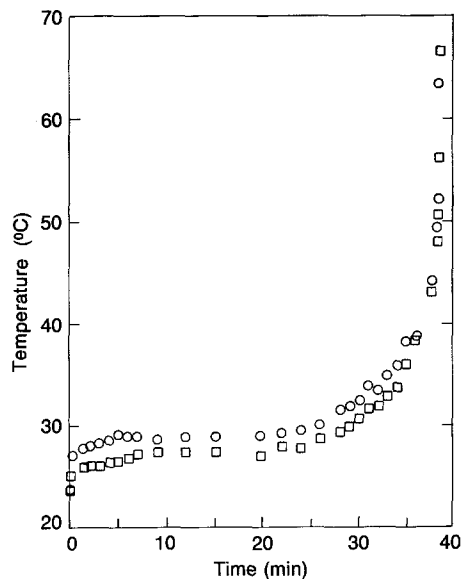


Figure 8 Temperatures measured at the fatigue crack tip for unfilled nylon 66 at a loading frequency of 5 Hz. (○) Crack closed position, (□) crack open position of the fatigue cycle.

### 3.3. Crack growth-temperature profiles

The fatigue crack growth rates and corresponding crack-tip temperatures for injection-moulded nylon 66 at a loading frequency of 5 Hz are shown in Fig. 9 as a function of the oscillating stress intensity factor. It is immediately apparent that significant hysteretic heating occurred throughout the fatigue test with maximum temperatures being even above the glass transition temperature for the dry nylon (45°C). Because the glass transition temperature is known to represent a brittle-to-ductile transition in terms of the deformational response of the material, the temperature rise provides a ready explanation for the previously observed fatigue fracture mode transition during the test. Specifically the change in fracture surface appearance from the more brittle patchy structure at the start of the test (below  $T_g$ ) to viscous flow at the end of the test (above  $T_g$ ) is understandable. In fact the thermography data exhibit three dis-

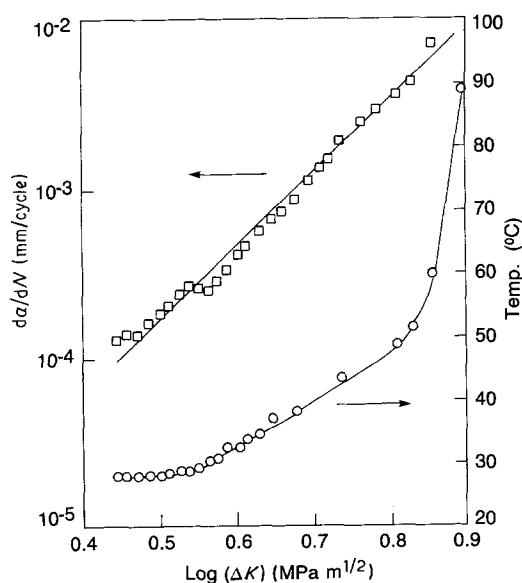


Figure 9 Comparison of fatigue crack propagation rates and crack-tip temperatures as a function of the oscillating stress intensity factor for nylon 66 at a frequency of 5 Hz.

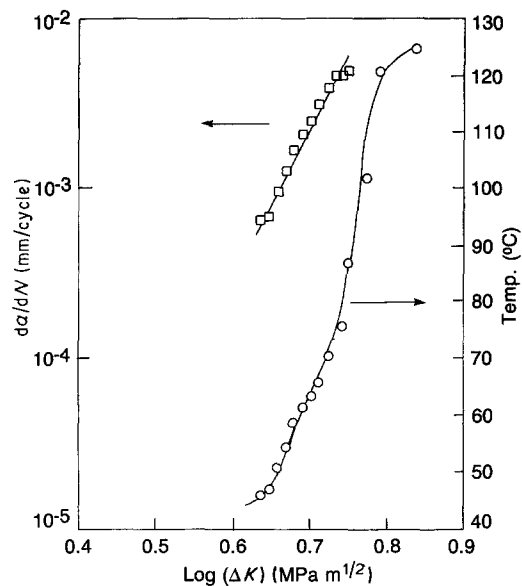


Figure 10 Comparison of fatigue crack propagation rates and crack-tip temperatures as a function of the oscillating stress intensity factor for nylon 6 at a frequency of 5 Hz.

tinct regions, an initial isothermal condition, a region of moderate temperature increase, and a region of more rapid heating at the termination of the test. This correlates well with the three distinct regions observed on the fracture surface of the nylon 66. From this comparison one can associate the patchy structure with room-temperature fatigue fracture, the more classical fatigue striations with some degree of limited ductility at temperatures near the glass transition temperature, and the more taffy-like viscous flow with deformation at temperatures above  $T_g$ .

Results for nylon 6 are shown in Fig. 10. Once again a significant temperature increase is noted though both the rate of increase and the maximum value are significantly higher than for the nylon 66. The lack of any well-defined isothermal region for the nylon 6 material explains the mixed mode fracture surface for this sample where both patchy and striated features were observed together even near the start of the crack propagation experiment. The differences in the rate of hysteretic heating for the two different types of nylon are primarily attributed to their respective  $T_g$ s, because the nylon 6 in the dry condition exhibits a  $T_g$  of only 40°C. The results of previous investigators also make it clear that the specific dynamic mechanical properties of the two materials will dictate their degree of hysteretic heating although such measurements were not a part of this study [12]. The crack growth rate data shown for nylon 6 in Fig. 10 can be easily described by the Paris type plot. There appears to be reduced data scatter compared to Fig. 3; however, a more limited range of  $\Delta K$  was covered in the measurements shown in Fig. 10. The comparison also serves to point out that a deceleration in crack growth rate due to hysteretic heating occurred at the higher  $\Delta K$  levels just prior to fast fracture. Presumably this reflects crack-tip blunting rather than a true effect of temperature.

The prior literature points to the use of lower frequencies as a means of reducing the influence of crack-tip heating during fatigue. This factor was confirmed in the present case as shown in Fig. 11 for nylon

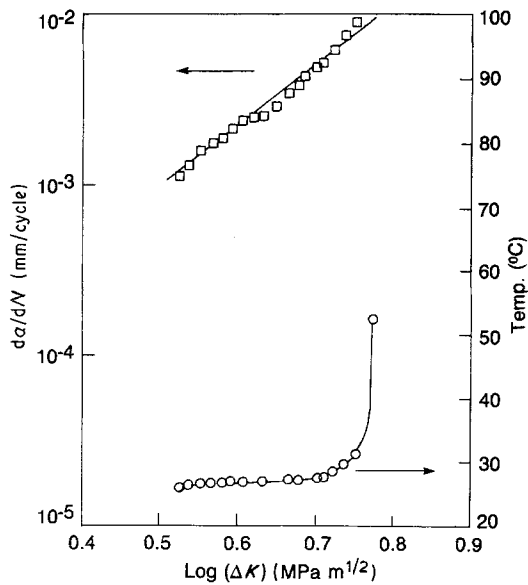


Figure 11 Comparison of fatigue crack propagation rates and crack-tip temperatures as a function of the oscillating stress intensity factor for nylon 66 at a frequency of 0.5 Hz.

66 at a reduced frequency of 0.5 Hz. At this frequency the temperature remains relatively constant until the end of the stable crack growth region. In fact, repeated experiments demonstrated that in many cases the sample undergoes catastrophic rupture before any detectable temperature rise occurs.

Samples which were fatigue fractured at the lower frequency of 0.5 Hz were examined to confirm the relation between fracture surface morphology and hysteretic heating. As shown in Fig. 12a, the patchy structure characteristic of fatigue fracture at

room temperature was observed over the first part of the stable crack growth region with no evidence of the striations noted at a frequency of 5 Hz. An abrupt transition to a taffy-like drawing of the nylon occurred at the end of the test (Fig. 12b) and this feature can be associated with the rapid temperature increase just prior to rupture (Fig. 11). These results demonstrate that the use of a lower frequency alone does not guarantee that valid crack propagation data will be obtained. For the results shown in Fig. 11 it is clear that the crack growth data at the end of the experiment should be ignored. As mentioned earlier, in some cases there is no evidence of a temperature increase at the lower frequency. In such cases the sample exhibits a patchy structure which undergoes a transition to fast fracture directly with no taffy-like region. This is shown in Fig. 12c. Ideally this is the type of fracture surface desired because it indicates that all of the crack growth data reflect a common fatigue fracture mechanism.

### 3.4. Effect of frequency

A comparison of the crack growth results in Figs 9 and 11 indicates that the fatigue crack grew faster at the lower frequency. Although it might be suspected that this effect was a result of the hysteretic heating, a close inspection of the thermography data (Fig. 9) shows that significant crack growth rate differences occurred even at the lower stress intensity levels where temperature increases were not observed. The influence of loading frequency was therefore further examined by making crack growth measurements at 0.1 Hz. The results are shown in Fig. 13 for all three frequencies. It is obvious that a strong frequency effect exists even under conditions (0.5 and 0.1 Hz) where no measurable hysteretic heating is occurring. The higher crack growth rates at lower frequency indicate that the time under load is a significant factor in the cracking kinetics. This dependence is more clearly illustrated by expressing the crack growth rate per cycle at a given level of stress intensity as a function of the time period of the oscillation,  $T$ , where  $T$  is equal to the inverse of the frequency in radians ( $2\pi$  times the frequency in Hz). This is shown in Fig. 14. The lowest possible

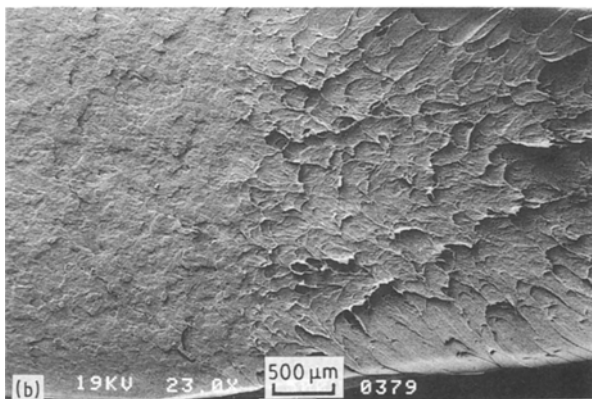
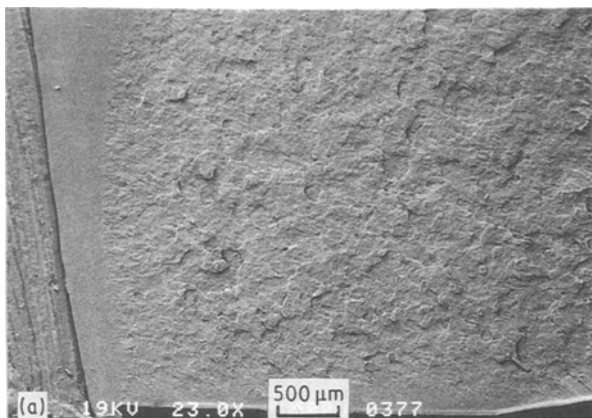


Figure 12 Fatigue fracture surface of nylon 66 tested at 0.5 Hz showing: (a) patchy structure at initiation, (b) patchy structure with transition to viscous flow just prior to termination and (c) patchy structure with abrupt transition at termination (fast fracture).

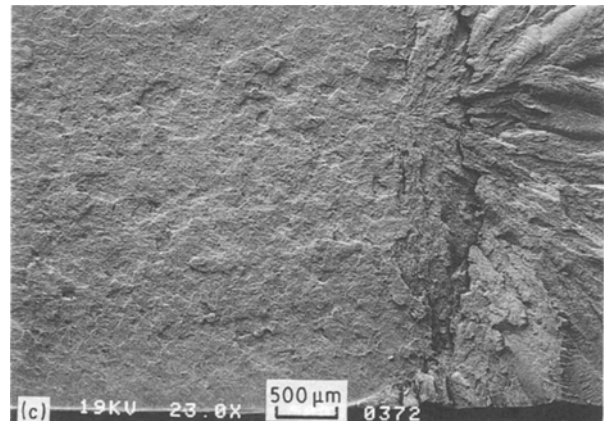
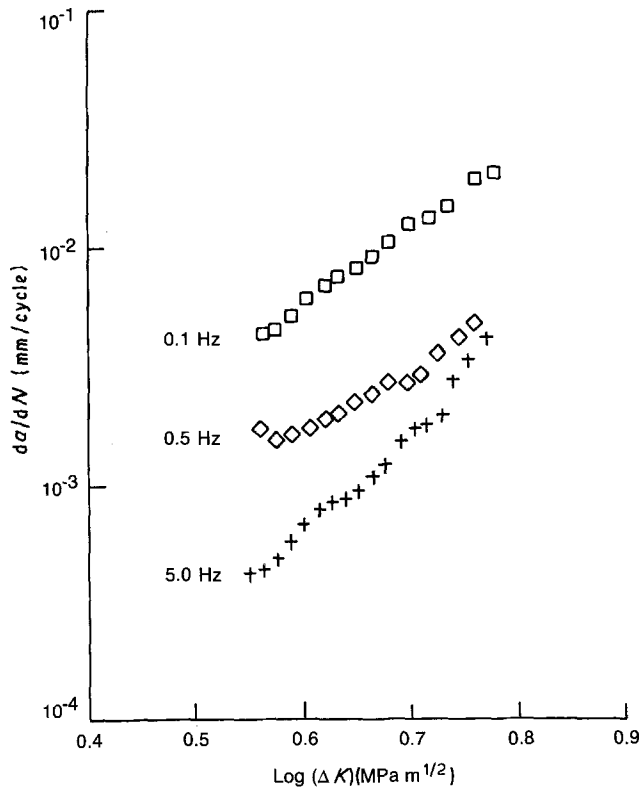


Figure 13 Effect of frequency on the fatigue crack propagation rates of unfilled nylon 66.



stress intensity level ( $\log \Delta K = 0.6$ ) was selected for the data shown in Fig. 14 in order to minimize any contribution from crack tip heating at the frequency of 5.0 Hz. The data clearly show a strong dependence of crack growth rate on time under load. This indicates that viscoelastic creep plays a major role in the fatigue crack propagation mechanism.

It is possible to quantify the results of Fig. 14 even further by considering that the fatigue crack growth is composed of two components [13]. One component is the crack growth due to a true fatigue process (i.e. each load cycle induces a certain amount of damage and consequent crack extension). The second component is the crack growth due to viscoelastic

creep which is proportional to the time under load. Mathematically this can be expressed as:

$$\frac{da}{dN_{\text{Total}}} = \frac{da}{dN_{\text{Fatigue}}} + \frac{da}{dt} \frac{dt}{dN}$$

Because  $dt/dN$  is equal to the time period of the cyclic oscillation, the intercept of the data in Fig. 14 represents the contribution due to true fatigue ( $0.6 \mu\text{m}/\text{cycle}$ ) while the slope ( $3.4 \mu\text{m}/\text{sec}$ ) represents the contribution due to creep. It is immediately apparent that at low frequencies the true fatigue contribution is very small for the nylon and most of the crack growth can be attributed to a creep process. For example, the crack growth rate at 0.1 Hz is approximately ten times

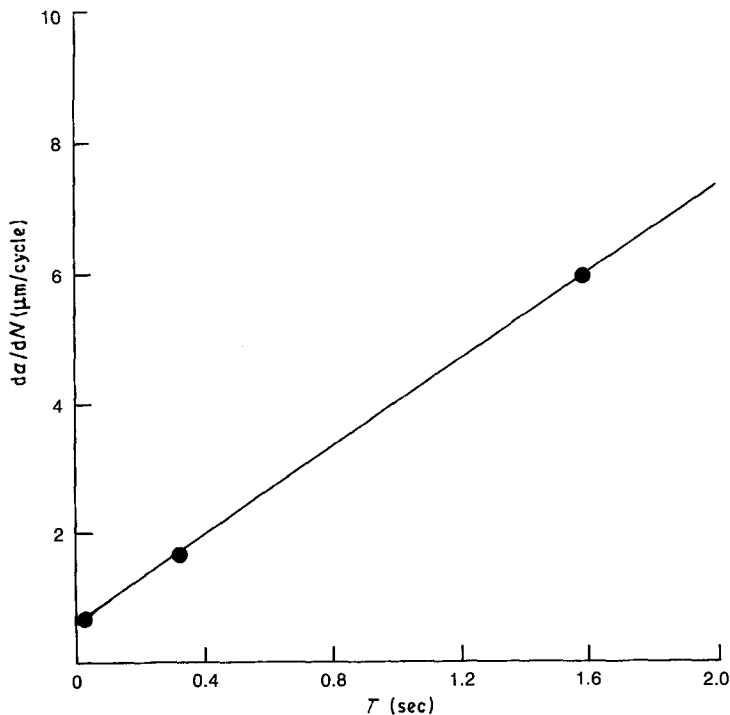


Figure 14 Fatigue crack propagation rates for unfilled nylon 66 plotted against time period of the oscillating load.



faster than that observed at 5 Hz. The linear relationship observed in Fig. 14 provides a possible means to quantitatively compare the creep-fatigue contributions to crack growth for various nylons. However, it should be kept in mind that any dependence on stress intensity level is ignored. Still, the analysis points out the order of magnitude of the creep contribution and the fact that, in the absence of creep, the fatigue crack growth rate would be greatly reduced.

#### 4. Discussion

Numerous accounts of cyclic stress-induced temperature increases can be found in the literature [10, 12, 14] and Hertzberg and co-workers, in particular, have described the hysteretic heating which occurs during fatigue fracture of nylon polymers [4, 12, 15]. The present study demonstrates that significant crack tip heating can occur even at relatively low frequencies and even for dry-as-moulded material. It was also shown that the fatigue fracture surface morphology changes in parallel with the temperature increases at the fatigue crack tip. However, the onset of measurable heating is not always reflected in the observed crack growth rate data and it is clearly possible to obtain Paris-type plots for data taken non-isothermally. Similarly it was shown that dramatic differences in the fracture surface can occur throughout the fatigue crack propagation measurement even though the data can be represented by a single line. The fractography does appear to provide a reliable method of verifying that a valid (isothermal) crack propagation test was performed. For the dry as-moulded nylon the characteristic patchy type structure should be observed from the initiation of fatigue cracking to the final catastrophic fracture at the termination of stable crack growth. The surface morphology changes which occurred during fatigue fracture at 5 Hz can generally be understood in terms of the ductile-to-brittle transition expected as the temperature increases above  $T_g$  due to hysteretic heating. However, the fractography results indicated that two transitions occurred with increasing temperature. First the patchy structure underwent a transition to the classical striated surface. The second change was the onset of viscous flow near the termination of the stable fatigue crack propagation region. The latter transition generally occurred when the crack tip temperature increased to above the glass transition temperature of nylon. The transition from a patchy structure to a striated surface is less clearly understood. It is a significant change because the fatigue crack tip extends more like a single entity with the growth involving the formation of a striation per each load cycle. This is suggested by comparing the striation spacing in Fig. 5c with the macroscopic crack growth rate ( $da/dN$ ) in Fig. 3. In contrast the patchy structure involves a variety of isolated regions where void and or craze formation has occurred and the effect of each loading cycle on crack tip advance is less obvious. The occurrence of surface striations during fatigue has previously been reported for moisturized nylons and thus one might expect that a slight temperature increase would produce a similar effect. The results of

this study suggest that as little as 10 to 20°C increase in temperature can cause the observed change. Presumably the onset of considerable shear yielding in the vicinity of the glass transition is the underlying cause of the change in crack propagation mechanism.

Although the occurrence of hysteretic heating and the fracture mode transition is of great interest, the objective of this study was also to define the effect of frequency in the absence of such heating. It is now clear that lower frequencies accelerate fatigue crack propagation rates in dry nylon. Furthermore, the representation of the crack growth rate data in terms of the time under load indicates that the extension of the crack tip is almost entirely due to a creep mechanism at these low frequencies. Previous investigators have suggested that viscoelastic creep may be contributing to the fatigue fracture mechanism and the similarity in fracture surface morphology for fatigue compared to constant load failures has also been noted [9, 13]. What is perhaps surprising is the magnitude of the creep contribution, especially considering that the measurements were made for dry nylon at room temperature.

In view of the extensive literature on nylon fatigue it is of interest to compare the results of the present study with those of others. This is especially important because there have been conflicting reports concerning the effect of frequency. Specifically it has been reported to have no effect and also to increase crack growth rates [8, 15]. In fact, for completely dry nylon, such as was used in this investigation, it has been reported that frequency has no effect [16]. This is contradicted by our results. The possible reasons for the discrepancy may relate to the specific frequency range investigated and also to sample thickness. For example, the possible reasons why thickness could influence the observed frequency sensitivity have been discussed by Lang *et al.* [15] and are consistent with the results presented here. In particular, a fatigue crack in a thinner plaque propagates under conditions closer to plane stress whereas thicker plaques approach plane strain crack propagation conditions. In terms of using crack propagation measurements to characterize fatigue resistance, the results of this study indicate that there is no unique  $da/dN-\Delta K$  relationship for thinner plaques. Although higher frequencies can be employed to minimize the creep contribution, as suggested by Fig. 14, it is likely that isothermal conditions will not be maintained due to hysteretic heating effects. This is currently being investigated along with the influence of sample thickness.

#### 5. Conclusions

1. Hysteretic heating causes fracture mode transitions to occur during fatigue crack propagation in injection-moulded nylons, even at relatively low (5.0 Hz) cyclic frequencies.
2. A strong frequency dependence exists for fatigue crack propagation even in the absence of hysteretic heating with higher crack growth rates at lower frequencies.
3. The frequency dependence indicates that the mechanism of fatigue crack propagation for dry nylon

at room temperature is primarily one of creep crack growth, especially at frequencies below 1.0 Hz.

### Acknowledgement

The authors thank Professor J. Gordon Williams, Imperial College, for helpful discussions concerning the effect of frequency on fatigue fracture.

### References

1. P. E. BRETZ, R. W. HERTZBERG and J. A. MANSON, *J. Mater. Sci.* **16** (1981) 2061.
2. *Idem, ibid.* **16** (1981) 2070.
3. R. W. LANG, J. A. MANSON and R. W. HERTZBERG, *Polym. Engng Sci.* **22** (1982) 982.
4. M. T. HAHN, R. W. HERTZBERG and J. A. MANSON, *J. Mater. Sci.* **21** (1986) 31.
5. J. F. MANDELL, F. J. MCGARRY, D. D. HUANG and G. C. LI, *Polym. Compos.* **4** (1983) 32.
6. E. JINEN, *J. Mater. Sci.* **21** (1986) 435.
7. M. I. KOHAN (ed.), "Nylon Plastics" (Wiley-Interscience, New York, 1973) p. 360.
8. R. W. HERTZBERG and J. A. MANSON, "Fatigue of Engineering Plastics" (Academic Press, New York, 1980).
9. D. C. MARTIN, G. E. NOVAK and M. G. WYZGOSKI, *J. Appl. Polym. Sci.*, **37** (1989) 3029.
10. R. N. HAWARD, "The Physics of Glassy Polymers" (Wiley, New York, 1973) p. 353.
11. R. W. LANG, M. T. HAHN, R. W. HERTZBERG and J. A. MANSON, *J. Mater. Sci. Lett.* **3** (1984) 224.
12. M. T. HAHN, R. W. HERTZBERG, J. A. MANSON, R. W. LANG and P. E. BRETZ, *Polymer* **23** (1982) 1675.
13. R. W. HERTZBERG, J. A. MANSON and M. D. SKIBO, *Polym. Engng Sci.* **15** (1975) 252.
14. R. ATTERMO and G. OSTBERG, *Int. J. Fract. Mech.* **7** (1971) 122.
15. R. W. LANG, J. A. MANSON and R. W. HERTZBERG, in "The Role of the Polymeric Matrix in the Processing and Structural Properties of Composite Materials", edited by J. C. Seferis and L. Nicolais (Plenum, New York 1983) p. 377.
16. R. W. HERTZBERG, M. D. SKIBO, J. A. MANSON and J. K. DONALD, *J. Mater. Sci.* **14** (1979) 1754.

*Received 12 April  
and accepted 28 September 1989*